Tr. J. of Physics
23 (1999) , 529 – 538.
© TÜBİTAK

Electrons and Phonons in GaN Semiconductor Quantum Well Devices

M. BABIKER, N. A. ZAKHLENIUK, C. R. BENNETT, V. N. STAVROU, B.K. RIDLEY
Department of Physics, University of Essex, Colchester CO4 3SQ, ENGLAND

Received 01.03.1999

Abstract

Electrons and polar optical phonons and their interactions are considered in the context of semiconductor quantum well devices, with particular reference to real quantum well laser structures. Distinction is made between wide-barrier and narrow-barrier structures and we explore the implications of these regimes for the description of the electron capture process. Special emphasis is made on the significant effects arising from the large effective mass ratio in AlN/GaN structures.

1. Introduction

The physics of semiconductor nano-devices, in particular double heterostructure quantum well (QW) lasers, is influenced significantly by the interaction of electrons and holes with the lattice vibrations of the heterostructure. Such interactions govern energy and momentum relaxation processes which determine carrier mobility and so underpin the quality of performance and speed of the device. This paper is concerned with the description of some of the carrier energy relaxation effects which are mediated by the exchange of polar optical (PO) phonons in a real QW laser structure. We examine the electron states and the phonon modes for typical parameters and typical device dimensions. In the case of electrons we highlight the important role played by the effective mass ratio, shown to be most prominent in the context of GaN/AlN QW systems. As for the PO phonons, we contrast the types of mode and their role in electron transitions using two phonon models: the bulk phonon model and the dielectric continuum (DC) model. A particular type of inter-subband process that we focus on in this context is the capture of electrons into the QW, specifically the capture of those electrons that are electrically injected or optically excited into the barrier region. It is well known that it is the captured electrons that must attain the population inversion responsible for the lasing action. We distinguish

between two physical situations: one consistent with narrow-barrier structures and the other consistent with the opposite case of wide-barrier structures.

2. Electrons

The electron motion is quantized whenever the corresponding de Broglie wavelength at typical electron energies is comparable to the dimension of the region in which the electrons are confined. In most of the real semiconductor device microstructures the confining potential is created by the energy band edge discontinuities at the interfaces between different materials. Usually the magnitude of this discontinuity is quite large (on the order of a few hundred millielectron-volts for GaAs/AlAs structures and about 2 eV for GaN/AlN structures). As a result of this the confining potential can be regarded as an infinitely deep square QW. However, this interpretation is relevant mainly when one is concerned with the electronic phenomena for which only the two-dimensional (2D) bound states of the electrons in the QW are important. There are other phenomena, such as real space transfer and electron capture in QW laser structures, for which both the electron states in the QW region and in the barrier region are equally important. In this paper we are interested in the electron relaxation effects due to the interaction with PO lattice vibrations which mediate the electron transitions between the QW bound states (in calculating the electron scattering rates of 2D electrons) as well as the electron transitions from the state above the confining QW potential to the bound states in the QW (in calculating the electron capture parameters). In the latter case, the description of the electronic states in the barrier region depends on the ratio between the width of the barrier layer and the de Broglie wavelength. For narrow-barrier structures the electron states in the barrier are also quantized if the outer confining potential is sufficiently high. In this case a coherent state for the electron is established within the whole structure (including the QW and the barrier region) and such a state is characterised by zero probability flux along the direction perpendicular to the QW interfaces. In the opposite case of wide-barrier structures with no confining outer potential the electron states in the barrier can be considered as true three-dimensional (3D) states (plane waves) with a non-zero probability flux.

In order to describe the above mentioned cases we consider the structure shown in Figure 1. The central QW, made of material 1, occupies the region $|z| < L$. This is sandwiched between two barrier layers made of material 2 of width D-L so that the conduction band offset amounts to a QW depth U_0. The magnitude of the potential U_0 will be considered in our calculations as finite or infinite, depending on the physical situation. Similarly, two cases will be considered for the outer confining potential U_1, namely: $U_1 = \infty$ and $U_1 = 0$. For the electron states we use the usual boundary conditions: continuity of the wavefunction Ψ and its derivative $(1/m_i^*)(\partial\Psi/\partial z)$ (m_i^* is the effective mass in material i) at the interfaces and zero wavefunction at the infinite barriers.

(i) *The case of a narrow-barrier structure.* Here, D is comparable to the de Broglie wavelength and $U_1 = +\infty$, i.e. the structure can be considered as a finite QW embedded

into an infinite QW. Solutions of the Schrödinger equation $\Psi(\vec{r}) = A_0^{-1/2}\Psi_k(z)\exp(i\vec{k}_\parallel\cdot\vec{\rho})$ subject to the boundary conditions gives rise to electron states $\Psi_k(z)$ that are symmetric,

$$\Psi_k^{(s)}(z) = C_s \begin{cases} sinh[k_2(D-L)]\cos(k_1 z), & |z| \leq L, \\ \cos(k_1 L) sinh[k_2(D-|z|)], & L \leq |z| \leq D, \end{cases} \tag{1}$$

and antisymmetric,

$$\Psi_k^{(a)} = C_a \begin{cases} sinh[k_2(D-L)]\sin(k_1 z), & |z| \leq L, \\ sgn(z)\sin(k_1 L) sinh[k_2(D-|z|)], & L \leq |z| \leq D, \end{cases} \tag{2}$$

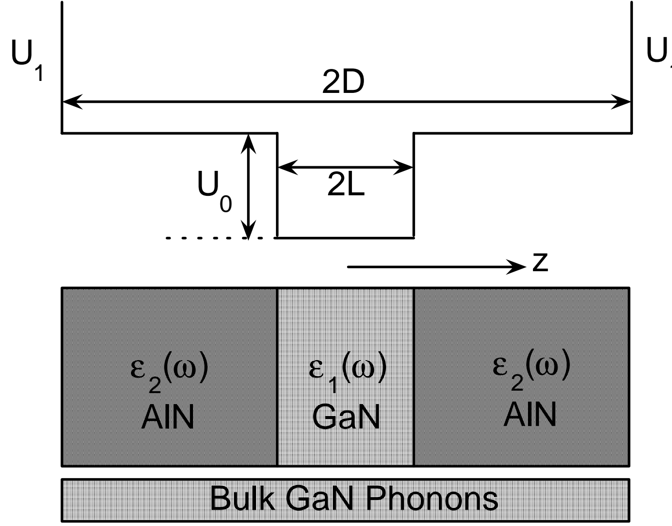

Figure 1. Schematic of the potential profile for electron confinement and the phonon system in a layered AlN/GaN quantum well structure ($\varepsilon_i(\omega)$ is the frequency-dependent bulk dielectric function in material i).

Here, $k_2 = \sqrt{2m_2^* U_0/\hbar^2 - m_2^* k_1^2/m_1^*}$, $C_{s,a}$ is a normalization factor, A_0 is the QW interface area, $\vec{\rho}$ is the in-plane position vector, sgn(z) is the sign of z and the total energy of the electrons is given by $\varepsilon_n\left(\vec{k}_\parallel\right) = \varepsilon_n + \hbar^2 k_\parallel^2/2m_1^*$ with $\varepsilon_n = \hbar^2 k_1^2/2m_1^*$, and $\vec{k}_\parallel$ is the in-plane wavevector. The value of k_2 is real when $\varepsilon_n < U_0$ and imaginary when $\varepsilon_n > U_0$. The dispersion relations for the symmetric and antisymmetric electron states are given, respectively, by

$$m_1^* k_2 \cos[k_1 L] cosh[k_2(D-L)] - m_2^* k_1 sin[k_1 L] sinh[k_1 L][sinh[k_2(D-L)] = 0 \tag{3}$$

$$m_1^* k_2 sin[k_1 L] cosh[k_2(D-L)] + m_2^* k_1 cos[k_1 L] sinh[k_1 L] sinh[k_2(D-L)] = 0. \tag{4}$$

Figure 2 shows the energy levels against half the well width L for the case $D = 600\mathring{A}$. It is seen that the energy levels outside the well form discrete subbands due to the presence of the outer infinite barrier and the subbands enter the well at near-regular intervals.

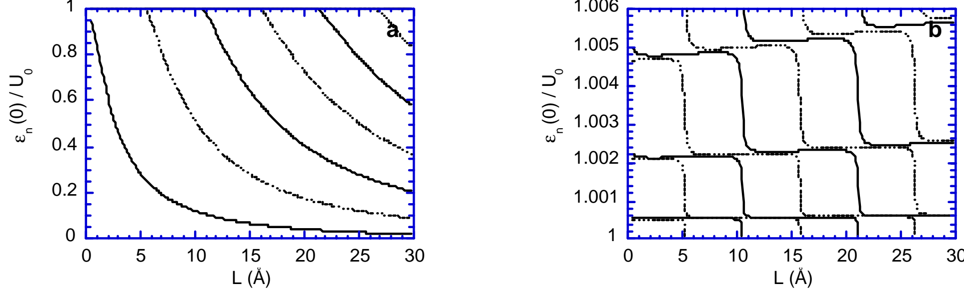

Figure 2. The electron energy levels for $k_\parallel = 0$ (a) within and (b) above the well. The solid curves are the symmetric states and the dotted curves the antisymmetric states.

(ii) *The case of infinite QW potential:* $U_0 = +\infty$. The electron states in this case can be obtained from the solutions in Eqs. (1)-(4) in the limit $U_0 = +\infty$. This gives a wavefunction equal to zero everywhere outside the QW and $\Psi_k^{(s,a)}(z) = C_{s,a}\cos(k_1 z)$ $(\sin(k_1 z))$ for the symmetric (antisymmetric) states in the QW with the energy levels obtainable from the relation $k_1 = n\pi/2L$ with $n = 0, 1, 2, \ldots$.

(iii) *The case of a wide-barrier structure with no outer potential:*$U_1 = 0$. The electron states above the barrier, with total energy $\varepsilon_n(\vec{k}_\parallel) > U_0$, correspond to a continuous spectrum (3D states). The electron wave undergoes partial reflection at the QW boundaries when it crosses the QW region. The resulting state is a superposition of incident and reflected waves. If we assume that the electron wave is incident from the left with an amplitude A then the wavefunction of the unbound states can be written as

$$\Psi_k(z) = A \begin{cases} e^{ik_2 z} + R_0 \exp\left[-i\left(k_2(z+2L) - \theta - \pi/2\right)\right], & z \le -L \\ Q_0^+ \exp\left[i\left(k_1(z-L) - k_2 L + \theta\right)\right] + & \\ Q_0^- \exp\left[-i\left(k_1(z-L) + k_2 L - \theta\right)\right], & |z| \le L \\ S_0 \exp\left[i\left(k_2(z-2L) + \theta\right)\right], & z \ge +L \end{cases} \tag{5}$$

where $R_0 = \frac{1}{2}T_0^{1/2}\left(\alpha\frac{\chi_1}{\chi_2} - \frac{1}{\alpha}\frac{\chi_2}{\chi_1}\right)\sin(\chi_1)$, $Q_0^\mp = \frac{1}{2}T_0^{1/2}\left(1 \pm \frac{1}{\alpha}\frac{\chi_2}{\chi_1}\right)$, $\tan\theta = \frac{1}{2}\left(\alpha\frac{\chi_1}{\chi_2} + \frac{1}{\alpha}\frac{\chi_2}{\chi_1}\right)\tan(\chi_1)$, $S_0 = T_0^{1/2}$, $\chi_{1,2} = 2k_{1,2}L$, and $\alpha = \frac{m_2^*}{m_1^*}$. The corresponding eigenenergy is given by $\varepsilon_n(\vec{k}_\parallel) = \varepsilon_2 + \varepsilon_\parallel^{(2)} = \varepsilon_1 + \varepsilon_\parallel^{(1)} - U_0$, where $\varepsilon_i = \frac{\hbar^2 k_i^2}{2m_i^*}$, $\varepsilon_\parallel^{(i)} = \frac{\hbar^2 k_\parallel^2}{2m_i^*}$, and k_i is the component of the wavevector along the z axis in the QW (i=1) and barrier (i=2) regions.

The electron transmission coefficient T_0 is given by

$$T_0 = \frac{\alpha u[1+u-(\alpha-1)u_{\parallel}]}{\alpha u[1+u-(\alpha-1)u_{\parallel}] + \left[\frac{\alpha+(\alpha-1)(u-\alpha u_{\parallel})}{2}\right]^2 \sin^2\left[\frac{\chi_0}{\sqrt{\alpha}}\sqrt{1+u-(\alpha-1)u_{\parallel}}\right]}, \quad (6)$$

where $u = \varepsilon_2/U_0$, $u_{\parallel} = \varepsilon_{\parallel}^{(2)}/U_0$ and $\chi_0 = \sqrt{8m_2^* U_0 L^2/\hbar^2}$. The important feature of Eq. (6) is that, due to the difference in the effective mass in the QW and barrier regions, the transmission coefficient depends explicitly on the free electron kinetic energy $\varepsilon_{\parallel}^{(2)}$ along the QW interfaces. If one uses the approximation $\alpha = 1$ this eliminates the dependence of T_0 on $\varepsilon_{\parallel}^{(2)}$, and the result is $T_0 = u(1+u)/\left[u(1+u) + (1/4)\sin^2\left(\chi_0\sqrt{1+u}\right)\right]$.

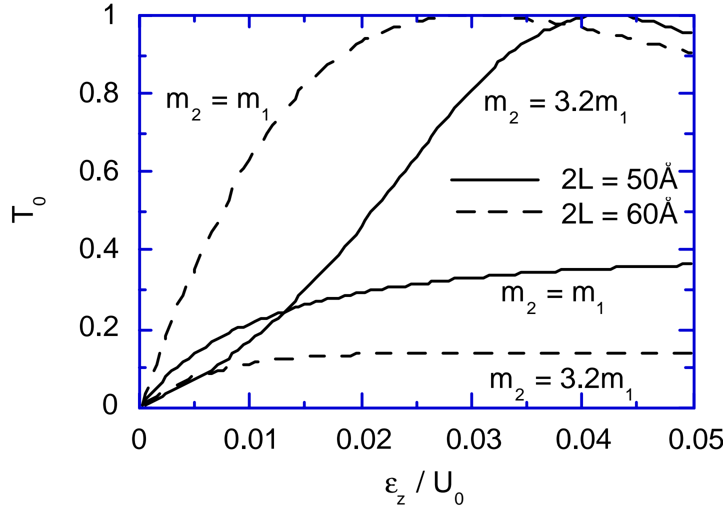

Figure 3. Transmission coefficient as a function of energy for a particular case $\varepsilon_z = \varepsilon_{\parallel}^{(2)}$ for two different QW widths.

As will be seen later, the explicit dependence of T_0 on $\varepsilon_{\parallel}^{(2)}$ has a strong effect on the electron-phonon interaction in the structure in question. In particular, for AlN/GaN structures the effective mass ratio is quite large, $\alpha = 3.2$, and this modifies significantly behaviour of T_0. Figure 3 shows the behaviour of T_0 for a particular case when the electron moves in the barrier region at an angle 45° towards the QW interface (in this case $\varepsilon_z = \varepsilon_{\parallel}^{(2)}$, where $\varepsilon_z \equiv \varepsilon_2$). Note that for the AlN/GaN structure $U_0 = 1.69\,\mathrm{eV}$ and the resonance energy, which corresponds to the maximum value of T_0, is zero ($\varepsilon_z = \varepsilon_{\parallel}^{(2)} = 0$) for the QW width 2L=48.65 $\mathring{A}$ and 2L=60.81 $\mathring{A}$.

The bound electron states below the barrier, with total energy $\varepsilon_n(\vec{k}_\parallel) < U_0$, can be presented as the superposition of a symmetric function,

$$\Psi_n^{(s)}(z) = C_n^{(s)} \begin{cases} \cos\left(\tilde{k}_1 L\right) \exp\left[-k_2\left(|z| - L\right)\right], & |z| \geq L \\ \cos\left(\tilde{k}_1 z\right), & |z| \leq L \end{cases} \tag{7}$$

and an antisymmetric function,

$$\Psi_n^{(a)}(z) = C_n^{(a)} \begin{cases} sgn(z) sin\left(\tilde{k}_1 L\right) \exp\left[-k_2\left(|z| - L\right)\right], & |z| \geq L \\ sin\left(\tilde{k}_1 z\right). & |z| \leq L \end{cases} \tag{8}$$

The dispersion equations for the eigenenergy $\varepsilon_n(\vec{k}_\parallel) = -\tilde{\varepsilon}_2 + \varepsilon_\parallel^{(2)} = \tilde{\varepsilon}_1 + \varepsilon_\parallel^{(1)} - U_0$, where $\tilde{\varepsilon}_i = \frac{\hbar^2 \tilde{k}_i^2}{2m_i^*}$, are given by $\frac{1}{\alpha}\frac{\tilde{\chi}_2}{\tilde{\chi}_1} = \tan\left(\frac{\tilde{\chi}_1}{2}\right)$ and $\frac{1}{\alpha}\frac{\tilde{\chi}_2}{\tilde{\chi}_1} = -\cot\left(\frac{\tilde{\chi}_1}{2}\right)$ for the symmetric and antisymmetric states, respectively. Figure 4 shows the energy levels for this case.

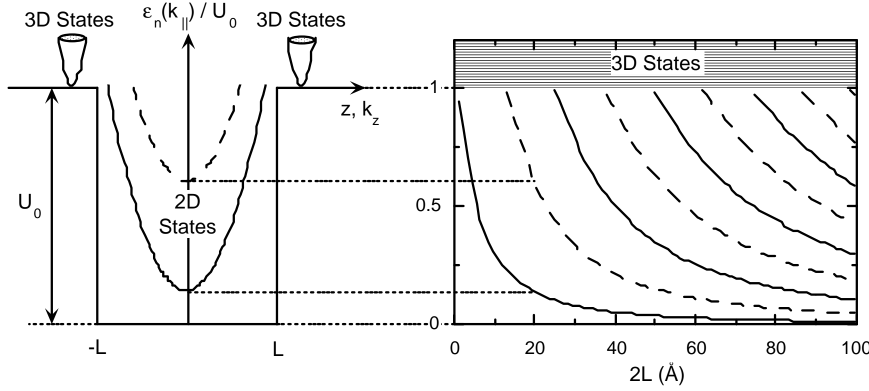

Figure 4. Electron energy levels of the symmetric (solid lines) and antisymmetric (dashed lines) states for structure with $U_1 = 0$ and $D \to \infty$.

The above electron states will be used in Section IV for the calculation of the electron-phonon interaction in the QW structures. In the next section we give a brief description of the PO phonon modes in the microstructures shown schematically in Figure 1.

3. PO phonons

The simplest approach for the description of the PO phonons in semiconductor microstructures is to use the bulk model in which one ignores the differences in the lattice properties of the materials constituting the microstructure. In this respect the structure

is considered as a homogeneous medium and the PO vibrations and the polarisation field potentials are described as plane waves, $\varphi_{\vec{q}}(\vec{r}) \propto e^{i\vec{q}\cdot\vec{r}}$, where $\vec{q}$ is a phonon wavevector. If the electrons are mainly confined within one of the layers then in the bulk phonon model it is usually assumed that the phonons in the whole structure are the same as in the bulk material of that layer. This is a reasonable physical model for the description of the electron-phonon interaction in microstructures with relatively thick QW layers when the QW width is larger than the phonon wavelength, or in structures with similar lattice properties of the layers. On the other hand, if the lattice properties of the layers are substantially different then it is obvious that the lattice vibrations in each layer will be modified by the presence of the neighbouring layers. In particular, if the eigenfrequencies of the PO phonons in the layers are substantially different then the phonons from one layer will not be able to propagate freely in the adjacent layer. This results in the phonon confinement effect. The simplest model which gives an account of the confinement effect is the dielectric continuum (DC) model [1, 2]. The DC model predicts three types of the PO phonons in microstructures: confined longitudinal (LO), confined transverse (TO), and the interface (IF) phonons. The corresponding polarisation field potentials within each layer can be presented in a general form as $\varphi_{\vec{q}_\parallel, q_z} \propto e^{i\vec{q}_\parallel\cdot\vec{\rho}}\varphi_{q_z}(z)$, where $\varphi_{q_z}(z) \propto cos(q_z z)$ $(\sin(q_z z))$ for the symmetric (antisymmetric) confined modes with quantized wavevector q_z, $q_z = \frac{\pi l}{2L}$, with l an integer, and $\varphi_{q_z}(z) \propto cosh(q_z z)\,(sinh(q_z z))$ for the symmetric (antisymmetric) IF modes. Exhaustive details of the calculation and quantization of the above phonon modes can be found in [2]. The peculiar feature of the DC model is that it completely ignores the bulk phonon dispersion. The description of the more elaborate hybrid model of PO phonons in microstructures is given in [3]. Our recent investigations [4, 5] show that in calculating total electron scattering rates, the DC model gives almost the same result as the hybrid model. The physical origin of this observation as well as comparison of the bulk phonon and DC model results for the electron-phonon relaxation rates will be discussed in the next section.

4. Electron-phonon interaction in microstructures

The main characteristic of many electronic QW microdevices is the electron transition rate. This indicates how in a given process the electron relaxes its momentum and energy, or how fast it is collected in a given final state. The electron transition rate determines both the electron mobility in the case of longitudinal transport along the QW and the electron population inversion in the case of the electron capture into the QW in laser microstructures [6, 7].

The spontaneous transition rate from the initial electron state $\Psi_i(\vec{r})$ into all possible final states $\Psi_f(\vec{r})$ mediated by the interaction with PO phonon modes is given by the Fermi Golden Rule,

$$\Gamma_i = \frac{2\pi}{\hbar}\sum_f\sum_\lambda |\langle\Psi_i(\vec{r})| - e\varphi_\lambda(\vec{r})\rangle|^2\delta(\varepsilon_i - \varepsilon_f - \hbar\omega_\lambda)\,. \tag{9}$$

where the index λ depends on the type of phonons. For bulk PO phonons $\lambda \equiv \vec{q}$;

for confined PO phonons $\lambda \equiv (\vec{q}_{\|}, l)$; and for IF PO phonons $\lambda \equiv \vec{q}_{\|}$. For bulk and confined PO phonons $\omega_\lambda = \omega_0$, where ω_0 is the LO frequency; for IF PO phonons $\omega_\lambda = \omega(\vec{q}_{\|})$, where $\omega(\vec{q}_{\|})$ is given by the corresponding dispersion equation [2]. We apply Eq. (9) for the calculation of the transition rates in AlN/GaN/AlN structure using the electron wavefunctions from Section II and the following material parameters: the electron effective masses are $m_1^* = 0.20m_0, m_2^* = 0.48m_0$; the low and high frequency dielectric constants are $\varepsilon_0^{(1)} = 9.5$, $\varepsilon_\infty^{(1)} = 5.35$, and $\varepsilon_0^{(2)} = 8.5$, $\varepsilon_\infty^{(2)} = 4.68$; and the LO frequencies are $\omega_0^{(1)} = 92.8$ meV and $\omega_0^{(2)} = 113$ meV.

(i) *Intra- and intersubband scattering rates of 2D electrons in a QW.* In this case we assume that the

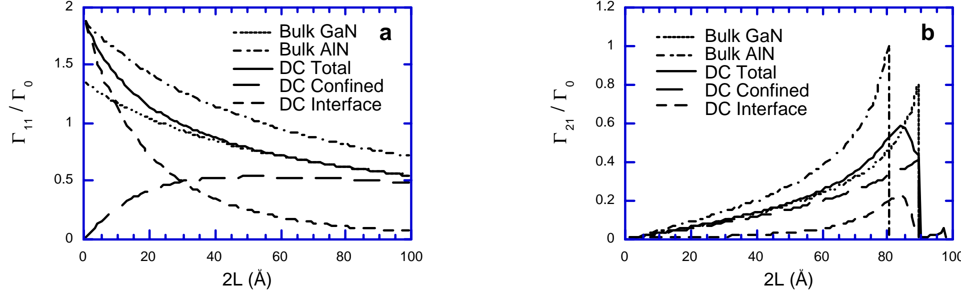

Figure 5. Intrasubband (a) and intersubband (b) scattering rates as a function of the QW width for different phonon models.

electrons are confined in an infinite QW and we use two phonon models, the bulk phonon model and the DC model. Figure 5 shows the scattering rate as a function of the QW width. Here, the parameter Γ_0 is $\Gamma_0 = (e^2/\hbar)\left(\varepsilon_\infty^{-1} - \varepsilon_0^{-1}\right)(2m_1^*\omega_0^{(1)}/\hbar)^{1/2}$ and the initial electron kinetic energy is $\varepsilon_{\|}^{(i)} = 2\hbar\omega_0^{(1)}$, in calculating the intrasubband scattering rate, and $\varepsilon_{\|}^{(i)} = 0$ (bottom of the second subband) for intersubband scattering. It can be seen from Figure 5 that the DC model result lies always between the results given by the GaN and AlN bulk phonon models. For a narrow QW the DC result is closer to the AlN bulk phonon result, while for a wide QW the DC result approaches the GaN bulk phonon result. This observation has a clear physical explanation connected with the change of the relative importance of the neighbouring layers with the change of the QW width. This result is very useful for estimating the scattering rates in real QW microdevices.

(ii) *Capture rate in a narrow-barrier structure.* The difference between the above calculation of the scattering rate in a QW and the calculation of the capture rate is that in the latter case the QW height is finite and the initial electron states are those with the energy above U_0 and the final states are below U_0. Using the wavefunctions from Section II we have calculated the capture rates for two phonon models: GaN bulk and DC. The

results are shown in Figure 6.

The capture rate exhibits the usual resonance-like behaviour [6, 7]. The important result of our calculation is that it indicates that the capture rates predicted by the bulk phonon model are quite close to those predicted by the DC model.

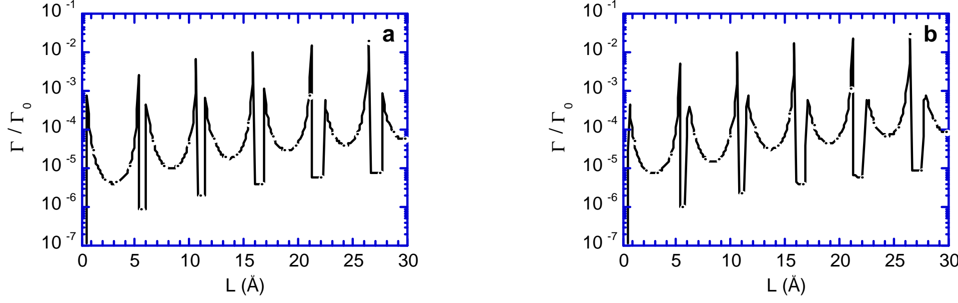

Figure 6. The bulk phonon (a) and DC phonon (b) mediated capture rate from the bottom of the first subband above the well vs half well width L.

(iii) *Electron capture in a wide-barrier structure.* In this case the initial electron state above U_0 lies in the continuous spectrum. The calculated capture rate is proportional to the intensity $|A|^2$ of the incident electron wave (see Eq. (5)). In order to obtain a relevant capture parameter for this case it is necessary to divide the capture rate by the intensity $|A|^2$. The result is the quantity $c(\varepsilon_z, \varepsilon_{\|}^{(2)})$ which has the dimensions of velocity and can be called a surface capture velocity from a given initial electron state $(\varepsilon_z, \varepsilon_{\|}^{(2)})$. We have calculated the capture velocity using the GaN bulk phonon model.

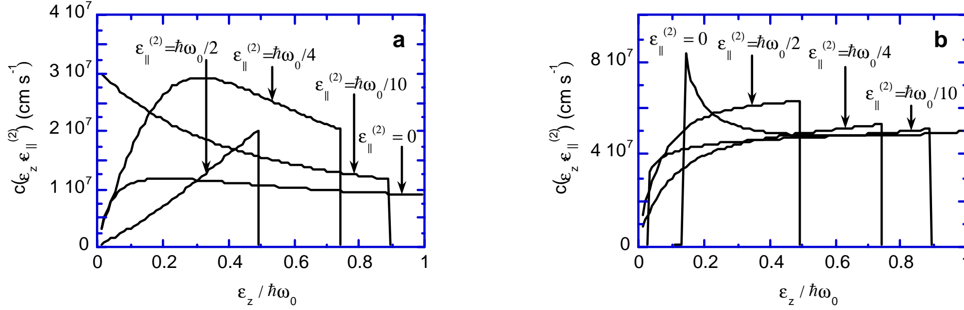

Figure 7. Capture velocity as a function of the kinetic electron energy ε_z for different values of the kinetic energy $\varepsilon_{\|}^{(2)}$ (as indicated) for two different QW width: (a) $2L = 49\mathring{A}$ and (b) $2L = 51\mathring{A}$.

Figure 7 presents the dependence of $c(\varepsilon_z, \varepsilon_{\|}^{(2)})$ for different values of $\varepsilon_{\|}^{(2)}$. As can be seen $c(\varepsilon_z, \varepsilon_{\|}^{(2)})$ is strongly affected by the values of $\varepsilon_{\|}^{(2)}$. As was discussed in Section II

this dependence is caused by the dependence of the transmission coefficient T_0 on $\varepsilon_{\|}^{(2)}$ due to the difference in the effective masses in the barrier and the QW regions .

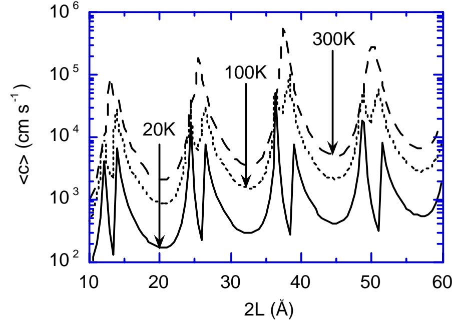

Figure 8. The average capture velocity as a function of the QW width.

Finally, Figure 8 shows the average capture velocity $< c >$ as a function of the QW width for different electron temperatures. The velocity $< c >$ was obtained by averaging $c(\varepsilon_z, \varepsilon_{\|}^{(2)})$ over the Maxwell-Boltzmann distribution function of the electrons in a continuous spectrum with electron temperature T.

The authors are grateful for support from the UK EPSRC (Grant GR/L56725) and the US Office of Naval Research (Grant N00014-96-1-0998).

References

[1] R. Fuchs and K.L. Kliewer, *Phys. Rev.,* **140A**, 2076 (1965).

[2] M. Babiker and N.A. Zakhleniuk, *Scattering of electrons by optical modes in bulk semiconductors and quantum wells, Chapter 6, in Hot Electrons in Semiconductors: Physics and Devices*, ed by N. Balkan (Clarendon Press, Oxford, 1998).

[3] B.K. Ridley, *Electrons and Phonons in Semiconductor Multilayers* (Cambridge University Press, 1997).

[4] C.R. Bennett, M.A. Amato, N.A. Zakhleniuk, B.K. Ridley, and M. Babiker, *J. Appl. Phys.,* **83**, 1499 (1998).

[5] V.N. Stavrou, C.R. Bennett, M. Babiker, N.A. Zakhleniuk, and B.K. Ridley, Phys. Low-Dim. Struct. **1/2,** 23 (1998).

[6] J.A. Brum and G. Bastard, Phys. Rev. B **33**, 1420 (1986).

[7] P.W. Blom, C. Smith, J.E.M. Haverkort, and J.H. Wolter, Phys. Rev. B **47**, 2072 (1993).